

중급물리실험1 – Single Photon Interference

배윤진

annieyon03@snu.ac.kr

Department of Physics and Astronomy, Seoul National University

(Dated: 2024-04-30)

Abstract

The interference–diffraction pattern are measured, and analyzed with fitting using various models for laser source. The Fraunhofer and Fresnel diffraction model are introduced. Same measurements taken for a bulb for the single photon interference regime. The linewidth of the each light source is calculated.

Keywords: Single Photon Interference; Fraunhofer diffraction; Fresnel diffraction

I. INTRODUCTION

With double slit interference experiment of Thomas Young in 1801, we could find that the light has wave nature. [1] Meanwhile, in 1905, Albert Einstein discovered the photo–electric effect, which showed the light also has particle nature. Additionally, it demonstrated the particle nature of light through the spectral distribution of blackbody radiation and Compton scattering. Through these findings, it is now understood that the particle and wave nature of light are essentially the same. This abstract also extends to particles like electrons or molecules, which can be conceptualized as waves, thereby linking to the idea of wave–particle duality. [2] – [4]

In this lab experiment, we investigated the double–slit interference–diffraction patterns in two different light sources. The first source is a monochromatic laser source, and the second source is nonmonochromatic bulb source. The laser source is used for the clear diffraction pattern, and the bulb source is used for the single photon interference regime. Under appropriate models for fittings, we aimed to analyze the interference–diffraction patterns of the light sources for several slits.

II. THEORETICAL BACKGROUND

A. Fraunhofer Diffraction

Generally the propagation of a wave follows the Huygens–Fresnel principle, where each point on a wavefront serves as a new source of wave. Among these, Fraunhofer diffraction occurs when the size of the slit is much smaller than the distance between the slit and the screen and light source. This condition can be written as (1), for the distance between light source and the screen L , the width of the slit W , and the wavelength of the light λ .

$$L \gg \frac{W^2}{\lambda} \quad (1)$$

In this case, the wave is consider as the plane wave, and the electric field of the wave at one point on the screen can be expressed as (2). E_0 is the amplitude of the wave, r_0 is the

distance between the source and the point, k is the wave number, w is the angular frequency, and t is the time. δ is the phase difference occurred from the position of each point source. [5]

$$dE = \frac{E_0}{r_0} e^{ikr_0 - wt} e^{i\Delta} \quad (2)$$

If we neglect the decrease in amplitude based on the r_1 and r_2 , which are the distance between each slit and the screen, we can write a intensity as (3) and (4) for single and double slits. In these equations, I_0 is the intensity of the light, a and b are the width of the slits, and h is the distance between the slits. And the θ is the angle between the normal line of the screen and the line connecting the point on the screen and the center of the slits.

$$I_{\text{single}(\theta, k)} = I_0 \frac{\sin^2(\beta)}{\beta^2}, \quad (3)$$

$$\beta = \frac{1}{2}ka \sin(\theta)$$

$$I_{\text{double}(\theta, k)} = \frac{I_0}{(a+b)^2} \left[a^2 \frac{\sin^2(\beta_1)}{\beta_1^2} + b^2 \frac{\sin^2(\beta_2)}{\beta_2^2} + 2ab \frac{\sin^2(\beta_1)}{\beta_1^2} \frac{\sin^2(\beta_2)}{\beta_2^2} \cos(2\alpha) \right], \quad (4)$$

$$\beta_1 = \frac{1}{2}ka \sin \theta, \beta_2 = \frac{1}{2}kb \sin \theta, \alpha = \frac{1}{2}kh \sin \theta$$

B. Fresnel Diffraction

If the conditions for Fraunhofer diffraction cannot be applied and nearer field conditions are used instead, this is referred to as Fresnel diffraction. In this case, the wave is not considered as a plane wave, but as a spherical wave. The electric field of the wave at one point can be expressed as (5), where r is the distance between the source and the point.

$$dE = \frac{E_0}{r} e^{ikr - wt} e^{i\Delta} \quad (5)$$

C. The diffraction pattern of non-monochromatic light

Typically, a light source is non-monochromatic, consisting a mix of various wavelengths. In non-monochromatic cases, the diffraction-interference pattern formula depends on the intensity of each wavelength of the light source. Using normalized spectral strength $g(k)$, we can calculate the intensity of the diffraction pattern of non-monochromatic light as follows:

$$I(\theta) = \int_0^\infty I_0(k) \left(\frac{\sin \beta(k, \theta)}{\beta(k, \theta)} \right)^2 \cos^2 \gamma(k, \theta) g(k) dk \quad (6)$$

Generally the spectral strength $g(k)$ follows the Lorentzian distribution. With the central value of the wavelength λ_0 and the standard deviation σ , the $g(k) = g(\frac{2\pi}{\lambda})$ can be expressed as follows:

$$g = \frac{2\sigma}{\pi((\lambda - \lambda_0)^2 + \sigma^2)} \quad (7)$$

III. METHODS

A. Experimental setup

The experiments were conducted using a Two-Slit Interference, One Photon at a Time educational kit of TEACHSPIN. The optical specifications of this kit is shown in the figure below.

Photomultiplier tube	Hamamatsu R 212
Preamplifier-Discriminator	Amptek A-111
Interference Filter	546 nm, 10 nm FWHM
Slit Widths	0.09 mm
Double-slit separations	0.35, 0.40, 0.45 mm
Laser	670 nm \pm 20 nm
Optical Path	1 m
Double-slit / Blocker slit distance	9.8 mm

Table 1. Optical specifications of the Two-Slit Interference, One Photon at a Time educational kit.

The path from a laser or light bulb through the slits the detector is called U-channel, which is shown in the figure below.

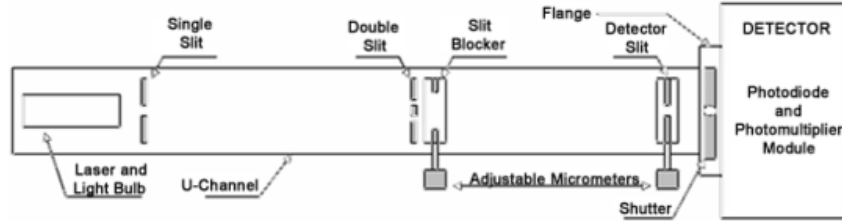


Figure 1. Schematic diagram of U-Channel. Adapted from [6].

The laser used as a lightsource has a wavelength of $\lambda = 670 \pm 20$ nm. The interference filter is 546 nm, 10 nm FWHM, and the optical light path is 1 m. The width of the slit is 0.09 mm, and the double slit separation is 0.35, 0.40, 0.45 mm.

Photodiode was used as a detector to detect the intensity of light while using the laser source. Meanwhile, PMT(Photon Multiplier Tube) was used as a detector to detect the photons while using the light bulb source, since the current of the light bulb is too weak to be detected by the photodiode.

B. Optical Alignment

For the experiment using laser source, all the optical alignment is done by checking the trajectory of the laser.

First the laser source is placed at the end of the U-channel, and the angle and the position is aligned to incide the light to the detector. Then the single slit near the laser source is placed to make the center of the light pass through the slit.

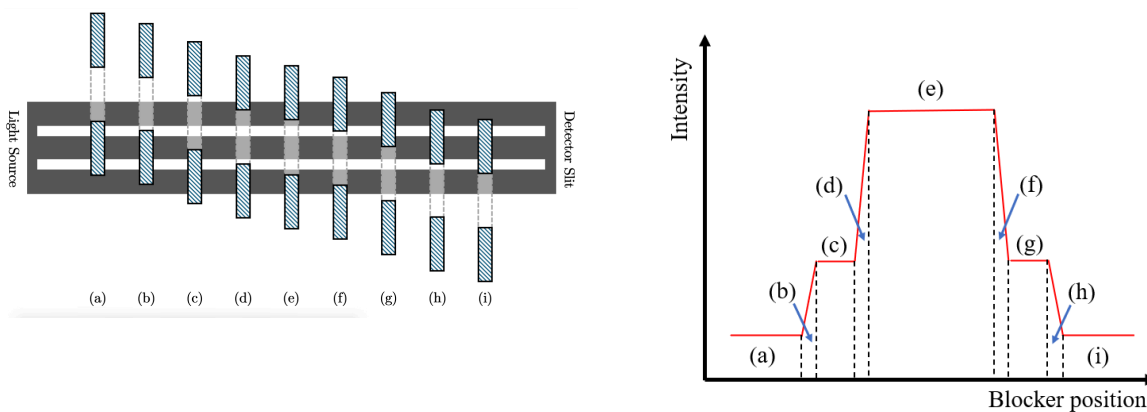
Next, the double slit is placed far from the single slit, and aligned to make a clear interference pattern. The blocker slit is then placed near the double slit. The blocker slit is used to block one of the slits to observe the interference pattern of the single slit, or the diffraction pattern of the asymmetric slit. Since the each shape of the slits in asymmetric slit should be the rectangular shape, it is necessary to check if the shape of the light emerging behind it changes symmetrically when the blocker slit is moved. Finally, the detector slit is aligned so that the shape of the light appearing on it matches the direction of the slit.

In experiments using bulb lightsource, unlike with lasers, observing the light's trajectory is challenging. Therefore, it is necessary to check the alignment position obtained in laser experiments, and then readjust from the beginning while monitoring the intensity of the light (number of signals) detected by the PMT.

C. Experiment with Laser source

1. Changing position of the blocker slit

After aligning, the blocker slit is moved and the voltages are measured. Each voltage is measured for every 0.05 mm. In this experiment, the micrometer should be moved slowly and not rotated in other direction, to prevent the backlash of the micrometer. These considerations are impertaive not only for this experiment but also in other experiments involving the adjustment of micrometer.



(a) Schematic diagram of the position of blocker slit and the double slit. (b) The Intensity of the incoming light for each position of the blocker slit.

Figure 2. Schematic diagram of the blocker slit position and the intensity. The same symbol from (a) to (i) indicates the same position of the blocker slit.

For accurate measurements, initially position the detector's micrometer at approximately 5.0 mm, which is considered the center, and vary the position of the blocker while recording the photodiode voltage. Figure 2 sequentially illustrates the relative positions of the blocker slit with respect to the double slit. This allows for verification of how much the double slit is obscured at each blocker position. It is anticipated that the voltage will display a slightly inclined step-like graph as each slit opens and closes. The segment where the voltage remains highest, presumed to be the double slit configuration, corresponds to section (e), while the second highest voltage sections, assumed to be the single slit configuration, are identified as (c) or (g). The intervals where the voltage changes abruptly, considered as the asymmetric double slit configurations, are identified as (d) and (f).

2. Symmetric double slit

Following the mentioned method to adjust the blocker slit for a double slit configuration, the detector slit is moved from 1 mm to 9 mm in increments of 0.05 mm, while the voltage is measured. This procedure is repeated for slits numbers 14, 15, and 16.

3. Single slit, Asymmetric double slit

After adjusting the position of the blocker to create single and asymmetric double slit configurations, the interference and diffraction patterns are measured. This experiment is conducted solely with slit number 14.

D. Experiment with Light bulb source

1. Finding the Optimal operating voltage range for PMT

PMTs operate with an adjustable driving voltage, which can be tuned to optimize their performance. In the absence of light, it is essential to ensure no counts, to minimize noise influence. With the bulb turned off, adjust the PMT's driving voltage while monitoring the number of pulses. By this method, the upper limit of the PMT driving voltage is determined through regression. Next, with a slight amount of light, the counts should begin to appear. For this purpose, set the bulb intensity to level 2 and adjust the PMT's driving voltage. Similarly, use regression to find the lower limit of the operating voltage.

Subsequently, set the PMT's driving voltage to the midpoint between the upper and lower limits, and adjust the threshold voltage to find the point where the number of PMT output pulses and PCIT pulses are similar.

2. Transfer function of the detector slit

This experiment is conducted before aligning the double slit with the blocker inserted. With the bulb intensity set to 5, the detector slit is moved from 1 mm to 9 mm in increments of 0.05 mm. This process allows for the determination of the transfer function of the detector slit. Additionally, by locating the detector position where the voltage peaks, the central point can be identified.

3. Measurement of PMT Pulse Counts Relative to Bulb Intensity

While incrementally increasing the bulb intensity from 1 to 5, the number of PMT pulses is measured. This experiment is conducted with the detector slit set at 5 mm.

4. Symmetric double slit & Single slit

After aligning the double slit with the blocker, the experiment proceeds with the bulb intensity set to 5. Ensuring that the blocker does not obstruct either of the two slits, the detector slit is moved from 1 mm to 9 mm in increments of 0.05 mm while measuring the number of pulses from the PMT. Slit number 14 is used for this part of the experiment to measure the interference pattern of a symmetric double slit.

Similarly, the experiment is repeated with the blocker obscuring one of the slits while leaving the other unobstructed. This setup allows for the measurement of the interference pattern of a single slit.

IV. RESULTS

A. Experiment with laser source

1. Changing position of the blocker slit

Each 14, 15, and 16 slits were aligned, and the intensity of left and right 1st order interference patterns were measured. Also the position of the blocker slit was changed and the voltage was measured. Those values were for the checking whether the slits are correctly aligned. The results are shown below. The peak difference is the difference between first left and right maximum intensity of the interference pattern. The visibility is the ratio of the first maximum and minimum intensity of the interference pattern. The blocker location indicates the position of the blocker at points (a) through (i) as shown in Figure 2.

slit	peak difference	visibility	blocker location [mm]
14	5.0 ± 0.5	3320.5 ± 8.5	2.45 2.60 2.80 2.95 4.20 4.45 4.55 4.75
15	5.2 ± 0.3	3595.0 ± 7.0	3.95 4.05 4.30 4.45 5.65 5.85 6.05 6.20
16	1.3 ± 0.2	4766.1 ± 28.2	3.55 3.65 3.95 4.15 5.2 5.35 5.65 5.75

Table 2. The peak difference of the 1st order interference pattern for slits 14, 15, and 16.

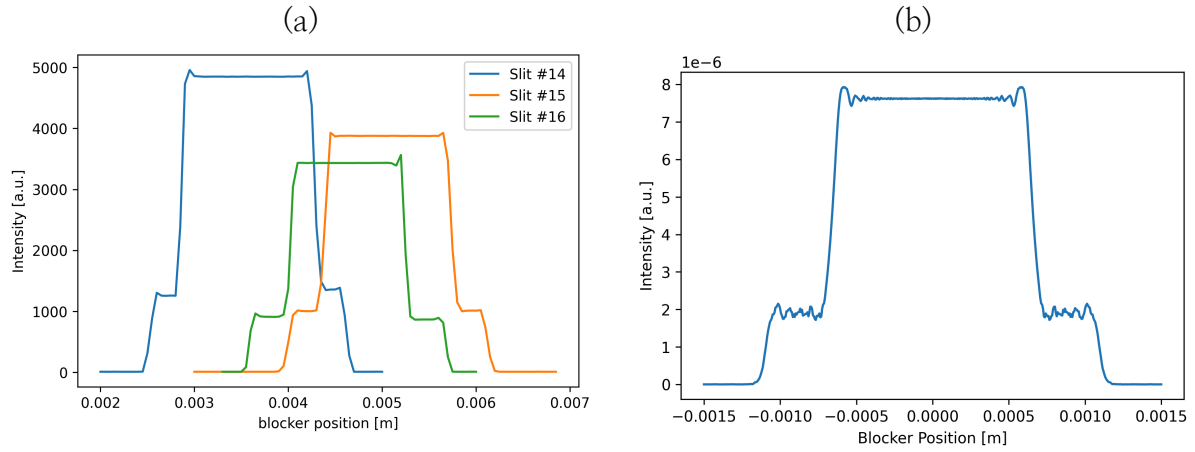


Figure 3. (a) The voltage measured for each position of the blocker slit for slits 14, 15, and 16. (b) The calculated intensity of the light for each position of the blocker slit.

In each graph in Figure 3, the central point of maximum intensity was recorded, and this information served as the basis for conducting subsequent experiments.

An interesting observation from the Figure 3 graph is that neither the experimental nor the theoretical data exhibit a perfectly angular shape. In the theoretical data, at points where the intensity rises to a low level, the intensity does not remain constant with the blocker position and shows significant noise. However, this is not as prominent in the experimental data. Nevertheless, at points where the intensity changes abruptly, a type of bump appears, which is consistently observed in both the theoretical and experimental data.

2. Symmetric double slit

The interference pattern of the symmetric double slit was measured for slits 14, 15, and 16. The results are shown in the figure below.

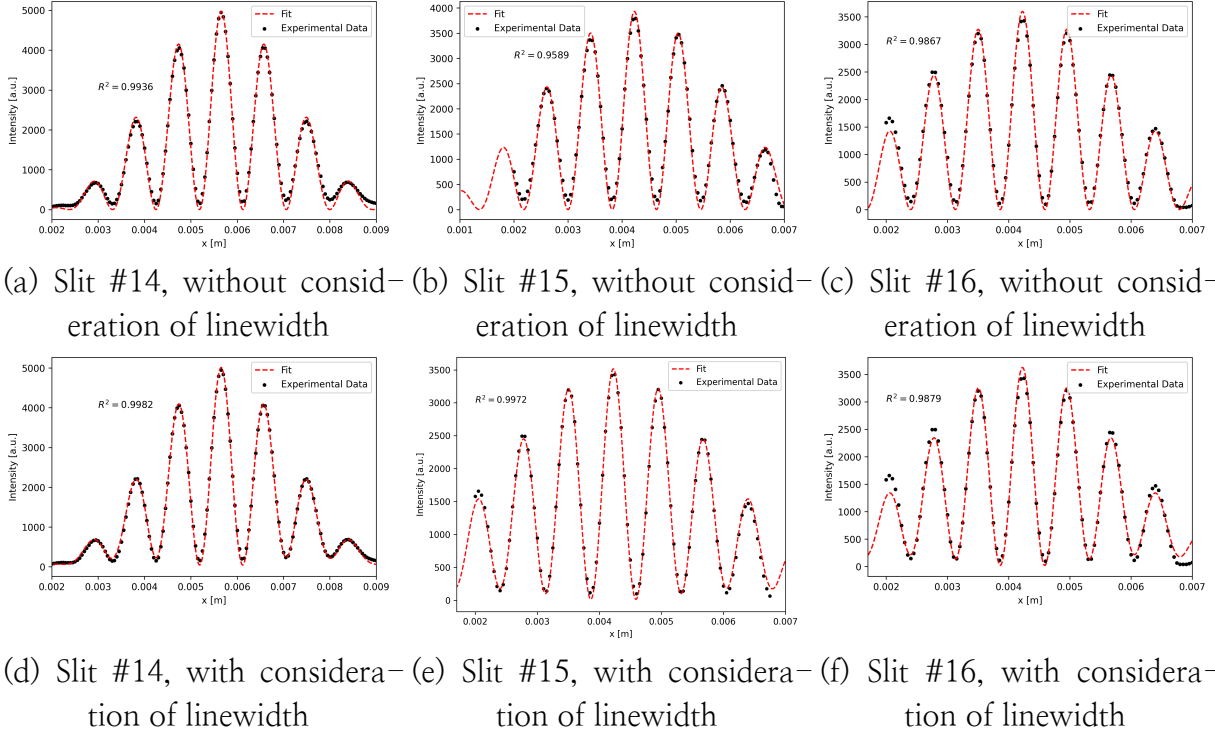


Figure 4. The interference pattern and the best fit of the symmetric double slit for slits 14, 15, and 16.

For (a) to (c) in Figure 4, the fitting was conducted without considering the wavelength linewidth. For (d) to (f), the fitting was conducted with consideration of the linewidth of wavelength. In the model that considering the wavelength linewidth, the central value of wavelength, λ_0 was fixed at 670 nm because the wavelength obtained from the model without considering linewidth was calculated with less than 1% error relative to λ_0 . In this model, the function of intensity respect to wavelength, $g(\frac{2\pi}{\lambda})$ was assumed to follow the Lorentzian distribution with standard deviation σ .

When considering the linewidth for each slit, it is observed that the R^2 values are higher compared to when linewidth is not considered, indicating a more accurate fit. This improvement is particularly pronounced towards the ends of the interference pattern. Comparing cases (a) and (d), in (a) it can be seen that there is a good fit at the minima near the center. However, around the detector position at $x = 0.008$ m in (a), the fitted graph does not align well with the experimental data, whereas in (d) there is a consistent match at all minima. Therefore, incorporating the wavelength linewidth into the model provides a significant improvement.

The variables obtained from the linewidth-considered model fitting are presented in the following table.

slit #	center position [mm]	width [μm]	distance between the slits [μm]	wavelength stdev. [nm]
14	5.656 ± 0.001	83.4 ± 0.5	356.4 ± 0.4	18.9 ± 0.4
15	4.228 ± 0.004	76.6 ± 2.0	408.1 ± 1.4	17.6 ± 1.7
16	4.227 ± 0.001	77.5 ± 1.0	457.1 ± 0.7	15.0 ± 0.8

Table 3. The variables obtained from the linewidth-considered model fitting.

3. The spectral density of the light source

As previously mentioned, the central value of the wavelength was fixed at $\lambda_0 = 670$ nm. Since the functions of intensity for each wavelength follows the same distribution for all slits, we can consider the standard deviation of the wavelength as the average of the standard deviations obtained from the fitting of each slit. Calculating this average, the standard deviation of the wavelength is $\sigma = 17.16$ nm. The spectral density of the light source is shown in the figure below.

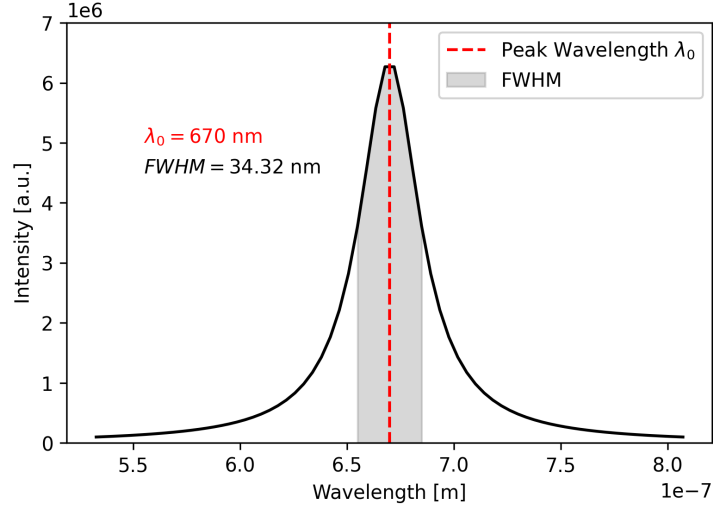


Figure 5. The spectral density of the laser light source.

Since the intensity of Lorentzian distribution becomes half at σ from the equation, the FWHM of the spectral density is $\text{FWHM} = 2\sigma = 34.32$ nm.

4. Asymmetric slit

The experimental data for the asymmetric double slit is shown in the figure below.

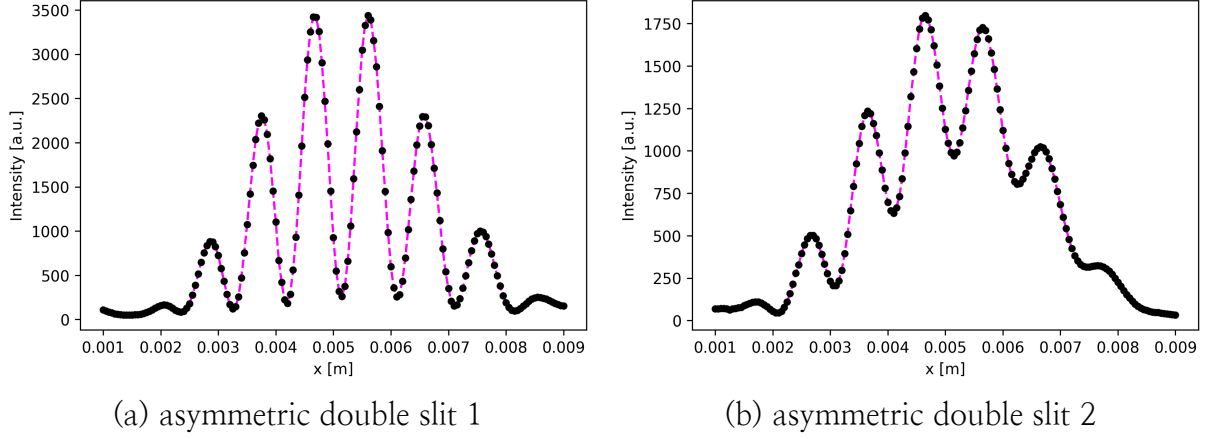


Figure 6. The experimental data for the asymmetric double slit for slit 14.

The fitting of the asymmetric double slit was conducted using two methods first. The first method, named A-Fitting, follows the model of (4).

However, A-Fitting assumes that the amplitudes produced at detector slit position x are always symmetrically centered. This can be easily shown by substituting θ into $-\theta$ in (4). This contradicts our experimental results that exhibit asymmetry. Thus A-Fitting can be considered as an unsuitable model. Consequently, it is necessary to attempt a fitting that considers the reduction in amplitude with the distances r_1 and r_2 from each slit to the screen. This method is referred as B-Fitting. However, the B-Fitting model also did not provide a satisfactory fit.

In B-Fitting, center position, width of one slit of double slit, and the distance between the slits were fixed at the values obtained from the symmetric double slit fitting. The ratio of the another slit's width to the width of the first slit was varied. The results shows all the data for varing the width of the other slit.

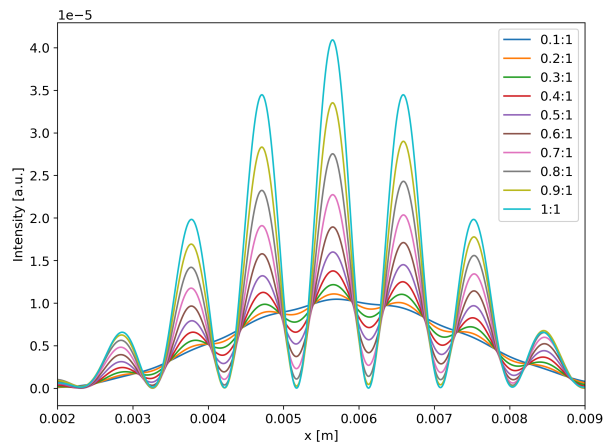


Figure 7. The interference-diffraction pattern calculated with B-Fitting model, varying the ratio of two widths of the slits.

Even the ratio of two widths was varied from 0.1 to 1.0, the calculated data does not match the experimental data, which was shown in Figure 6. For instance, in Figure 6 (a), two peaks of equal height should appear, yet this pattern is never observed in Figure 7. While B-Fitting has the advantage of being able to represent asymmetry compared to A-Fitting, it proved inapplicable to the actual experimental data. We will continue to investigate more suitable fitting models in discussion section.

5. Single slit

Similarly, for the single slit, both A-Fitting and B-Fitting approaches were attempted. The results obtained from A-Fitting are as follows. The wavelength linewidth was considered in the fitting. For each attempt, only the width of each slit d_1 and d_2 was varied, with other values were fixed at the values obtained from the symmetric double slit fitting.

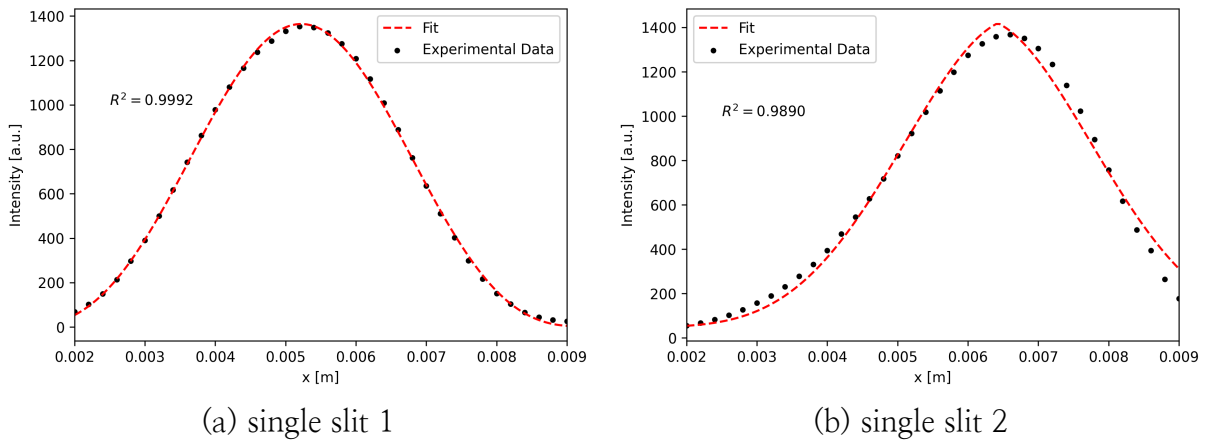


Figure 8. The diffraction pattern and the best fit of the single slit for slit 14. A-Fitting used.

The width for the first slit of double slit (that corresponds to Figure 8 (a)) was $d_1 = 84.8 \pm 0.1 \text{ } \mu\text{m}$. Also the second slit of double slit (that corresponds to Figure 8 (b)) was $d_2 = 84.6 \pm 0.1 \text{ } \mu\text{m}$.

Now, we can conduct a statistical test to determine if the two slits are of equal width. The difference between two slit widths was $d_1 - d_2 = 0.2 \text{ mm}$. The standard error σ for the difference between two independent variables with standard error σ_1 and σ_2 can be calculated as follows:

$$\sigma = \sqrt{\frac{\sigma_1^2 + \sigma_2^2}{2}} = \sqrt{\frac{0.1^2 + 0.1^2}{2}} = \sqrt{\frac{0.02}{2}} \simeq 0.10 \text{ mm} \quad (8)$$

Hence Z-score for the difference between slit widths is calculated as follows:

$$Z = \frac{d_1 - d_2}{\sigma} = \frac{0.2}{0.10} \simeq 2.00 \quad (9)$$

Typically, from two-tailed test, if a Z-score is greater than 1.96, the difference is considered significant. Here, the calculated Z-score is 2.00, which is greater than 1.96. Therefore, the null hypothesis is rejected under 95% confidence interval. This indicates that the two slits

are not of equal width. However, the fitting error σ is not same with the sample standard deviation, so the result should be interpreted with caution. For the better result, the error should be calculated from the independent measurements of the slit widths, and each fitting parameter.

B. Experiment with bulb source

1. Measurement of PMT Pulse Counts Relative to Bulb Intensity

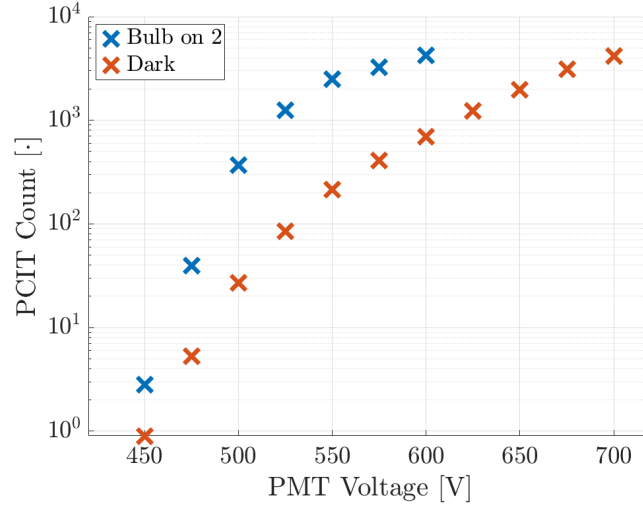


Figure 9. PCIT counts relative to the PMT voltage. Interval = 10 s

Figure 9 shows the number of PCIT counts relative to the PMT voltage in logarithmic scale, for the bulb intensity set to 2 and zero (corresponds to “dark”). The graph shows the logarithmic scale of the number of PCIT counts is increasing logarithmic relative to the PMT voltage again, so the PCIT counts increase in $\log(\log(V))$ scale. In theory, the PMT driving voltage can be determined as a value between the upper and lower limits, where both are found from the regression of the PCIT counts. However, since both graph shows a similar x-intercepts at around PCIT count 10^0 to 10^1 , and it is difficult to found the exact x-intercept since it does not show a clear linear relationship, we have to set the PMT driving voltage by other method.

Among this data, the greatest ratio of data was observed at the PMT voltage of $V_{\text{opt}} = 525$ V, where $\frac{N_{\text{intensity}=2}}{N_{\text{dark}}} = \frac{1245.5}{84.6} = 14.7$. This indicates that at this voltage, the difference in PCIT counts for the same bulb intensity is the most pronounced, implying that PCIT counts can be measured with increased sensitivity. Therefore, we have set the optimal PMT voltage at 525 V. At this voltage, the PCIT count for dark bulb in 10 seconds was 84.6 counts. Hence, it was determined that for the forthcoming second of experimnetation, 8.46 counts should be considered as noise and subtracted accordingly.

2. Transfer function of the detector slit

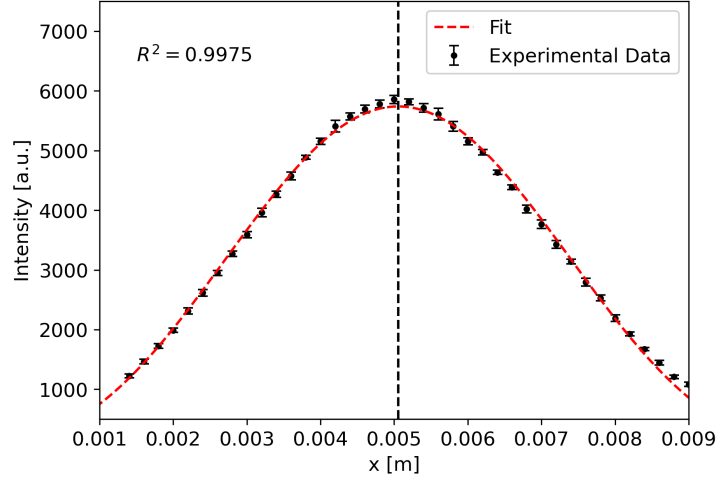


Figure 10. The intensity of the light (number of the signal) detected by the PMT while moving the detector slit.
The bulb power was set to 5.

After aligning the bulb, the intensity was measured by moving the detector, and the graph for Figure 10 was obtained without inserting the double slit. Fitting this data with a Gaussian function resulted in an $R^2 = 0.9954$, indicating high accuracy. The central value was determined to be $x = 5.05 \pm 0.010$ mm. This value was then used to set boundary of central value when fitting the double slit.

3. Pulse Count–Bulb Power Relationship

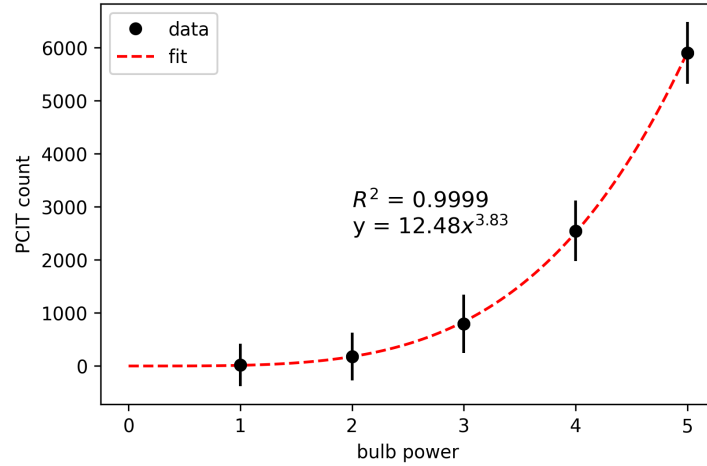


Figure 11. The number of pulses relative to the bulb power.

Fitting the pulse count and the bulb power into $y = ax^n$, we could find that $a = 12.48 \pm 0.92$, and $n = 3.82 \pm 0.04$. Substituting this, we can write the relation between the bulb power I and the pulse count N as

$$N = (12.48 \pm 0.92)I^{3.82 \pm 0.04} \quad (10)$$

4. Symmetric double slit

The interference pattern of the symmetric double slit in bulb source was also measured for slits 14, 15, and 16. The results are shown in the figure below.

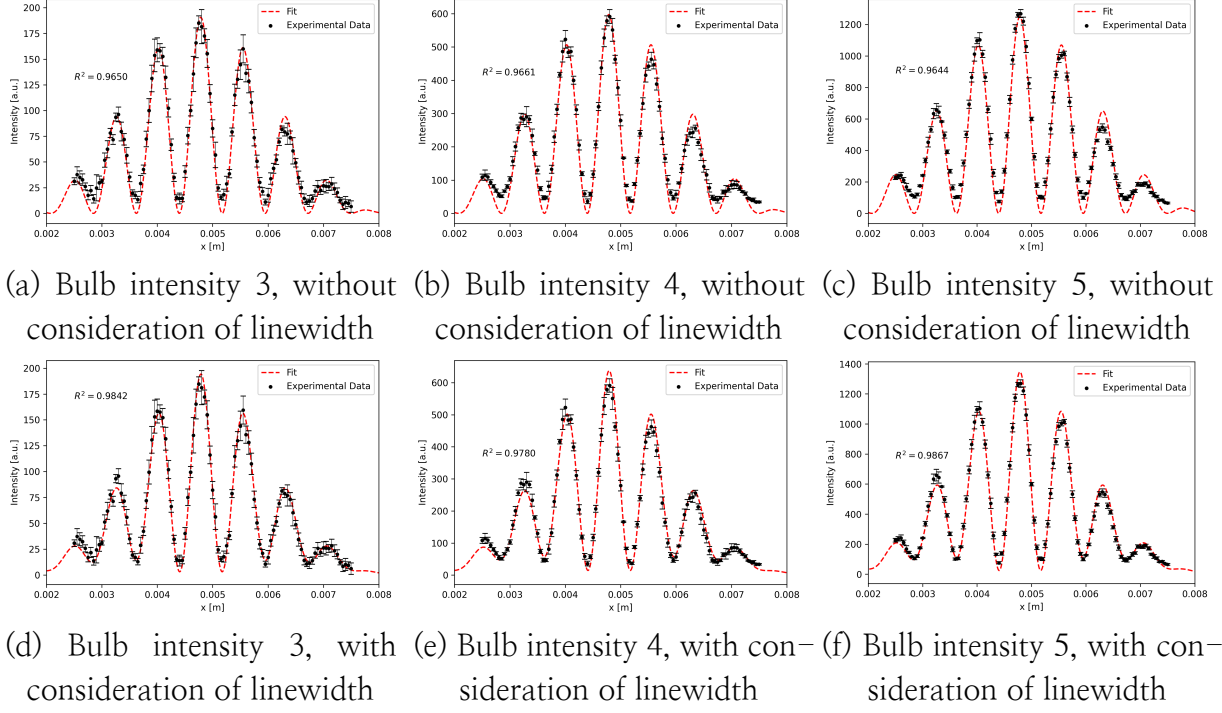


Figure 12. The interference pattern and the best fit of the symmetric double slit for bulb intensities 3, 4, and 5.

bulb intensity	center position [mm]	width [μm]	distance between the slits [μm]	wavelength [nm]	stdev.
3	4.786 ± 0.003	82.2 ± 1.7	364.8 ± 1.1	21.2 ± 0.8	
4	4.785 ± 0.002	81.8 ± 1.6	365.1 ± 1.1	25.4 ± 1.0	
5	4.776 ± 0.002	79.2 ± 1.8	364.2 ± 1.2	22.7 ± 2.8	

Table 4. The variables obtained from the linewidth-considered model fitting in bulb light source

Similar to the laser source experiment, fixing the center wavelength as $\lambda_0 = 567 \text{ nm}$, the standard deviation of the wavelength was calculated from the Table 4 value, as $\sigma = 23.1 \text{ nm}$. This value is quite bigger than the laser source, which was 17.16 nm . Applying this value to the Lorentzian distribution, the spectral density of the light source is shown in the figure below.

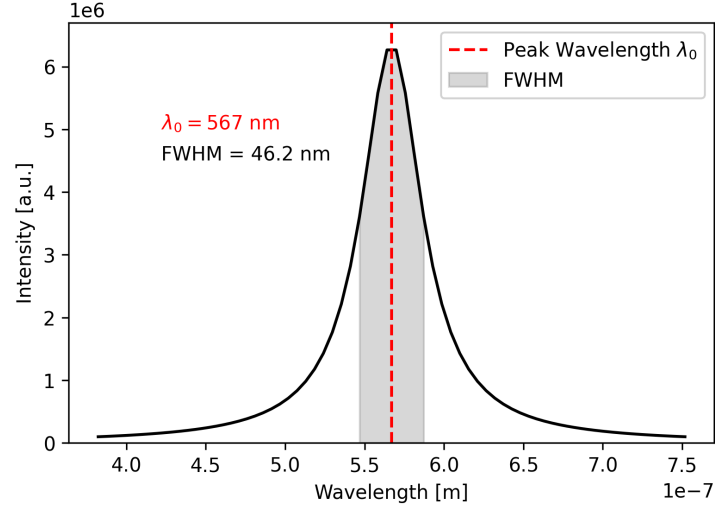


Figure 13. The spectral density of the bulb light source.

In the same way, the FWHM of the spectral density is $\text{FWHM} = 2\sigma = 46.2 \text{ nm}$.

5. Single slit

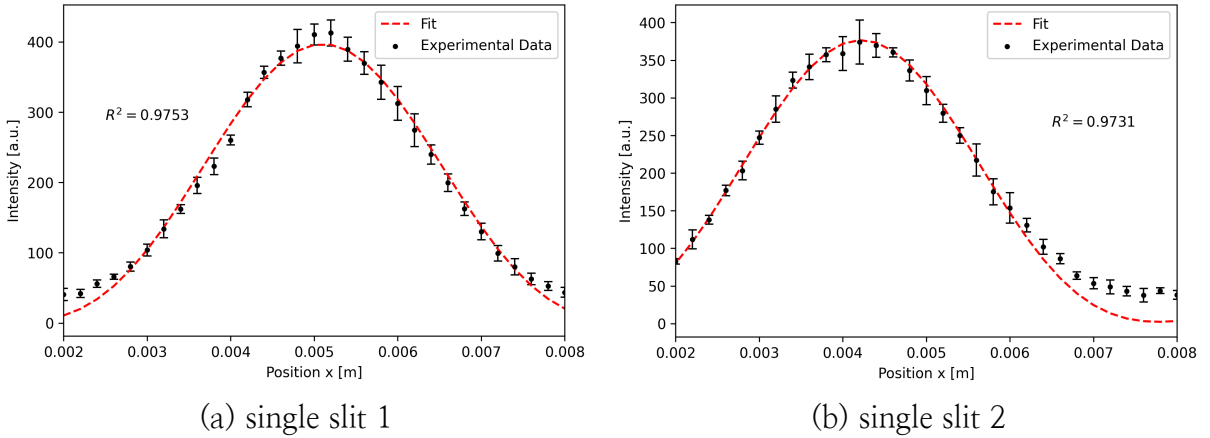


Figure 14. The diffraction pattern and the best fit of the single slit for slit 14, with bulb source. A-Fitting used.

The width for the slit 1 of double slit (that corresponds to Figure 14 (a)) was $d_1 = 79.8 \pm 1.7 \text{ } \mu\text{m}$. Also the slit 2 of double slit (that corresponds to Figure 14 (b)) was $d_2 = 80.5 \pm 1.8 \text{ } \mu\text{m}$.

Again, we can conduct a statistical test to determine if the two slits are of equal width. The difference between two slit widths was $|d_1 - d_2| = 0.7 \text{ } \mu\text{m}$. The standard error σ can be calculated as follows:

$$\sigma = \sqrt{\frac{\sigma_1^2 + \sigma_2^2}{2}} = \sqrt{\frac{1.7^2 + 1.8^2}{2}} = \sqrt{\frac{6.13}{2}} \simeq 1.748 \text{ } \mu\text{m} \quad (11)$$

Hence Z-score for the difference between slit widths is calculated as follows:

$$Z = \frac{|d_1 - d_2|}{\sigma} = \frac{0.7}{1.748} \simeq 0.400 \quad (12)$$

The calculated Z-score is less than 1.96, so we cannot reject the null hypothesis that the two slits are of equal width. Therefore, we can conclude that the two slits are of equal width. However, as mentioned in the laser source experiment, the fitting error σ is not same with the sample standard deviation, so the result should be interpreted with caution.

V. DISCUSSION

A. Discussion on Whether the Intensity of Light Passing Through the Two Slits is Equal

In this report, all fittings and models are predicated on the assumption that the intensity of light passing through the two slits of the double slit is equal. To discuss this, a table can be constructed based on the data from Figure 3 as follows.

slit #	Intensity at left horizontal region [a.u.]	Intensity at right horizontal region [a.u.]	difference ratio
14	1256.5 ± 2.5	1354.3 ± 5.5	$2.017 \pm 0.009 \%$
15	1003.0 ± 1.0	1011.0 ± 1.0	$0.206 \pm 0.000 \%$
16	910.3 ± 1.7	865.4 ± 1.5	$-1.305 \pm 0.003 \%$

Table 5. The variables obtained from the linewidth-considered model fitting.

The ‘difference ratio’ refers to the value obtained by dividing the difference in intensity between two small horizontal sections, which occurs when moving the blocker, by the intensity of the right horizontal section.

From the t-test, the T-statistic for the each two slits are -0.487 , and the p-value is 0.674 . This p-value is much greater than the significance level of 0.05 , so we cannot reject the null hypothesis that the intensity of light passing through the two slits is equal. Therefore, we can conclude that the intensity of light passing through the two slits is equal.

B. Asymmetric slit Fitting, with Fresnel diffraction model

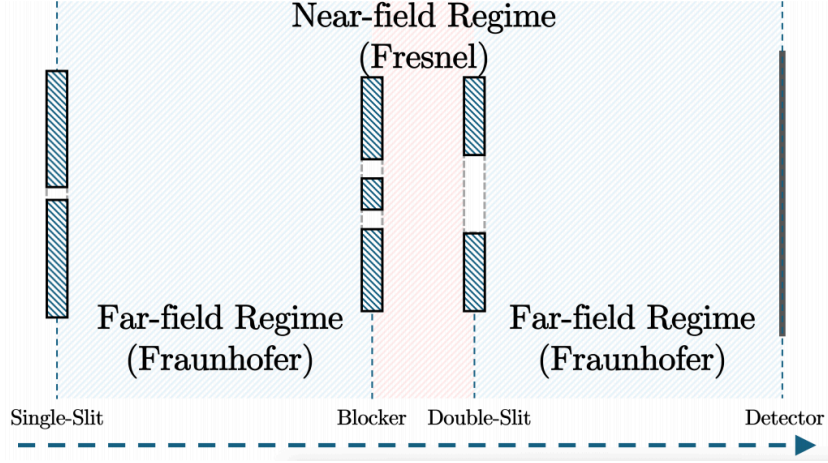


Figure 15. The far field and near field regions.

As mentioned in section IV.A.4, the fitting of the asymmetric double slit was conducted using two methods, A-Fitting and B-Fitting. However, neither method provided a satisfactory fit. Figure 15 shows why the far-field model is not applicable to the asymmetric double slit. The distance between the blocker and the double slit is about 1cm, and this should be considered as the near-field regime. For the symmetric double slit cases, this near-field regime does not matter since the optical path is passing the blocker completely between the end of the blocker slit. However, in the case of the asymmetric double slit, the optical path is affected by the blocker position, the Fresnel diffraction in this region becomes dominant.

For this reason, for the better fitting, we can consider the fresnel diffraction model. Though the fresnel diffraction model takes more time to calculate, it can provide a more accurate fitting.

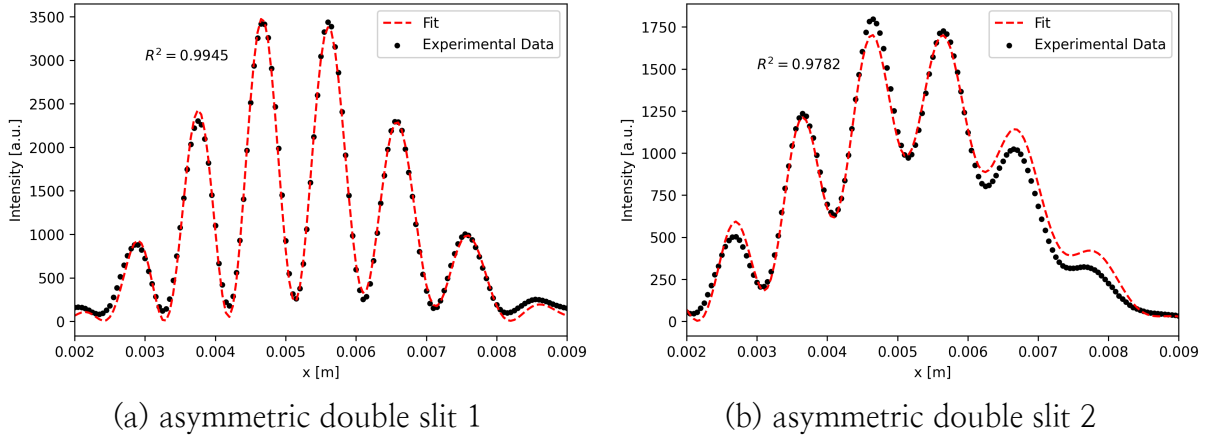


Figure 16. The experimental data for the asymmetric double slit for slit 14, with fresnel diffraction model.

From the asymmetric double slit fitting, we could find the width of the blocker slit, w and the position of the blocker, d . From the first asymmetric double slit, each value was $w_1 = 1.717 \pm 0.023$ mm, and $d_1 = 675.6 \pm 11.3$ μm . From the second asymmetric double slit, each value was $w_2 = 1.696 \pm 0.020$ mm, $d_2 = 709.3 \pm 9.9$ μm .

As seen in Figure 16, the fresnel diffraction model provides a better fit than the previous models, A-Fitting and B-Fitting. From this, we can conclude again that for the asymmetric double slit region, we cannot ignore the effect that comes from the distance between the slits and the screen, and the reduction in amplitude with the distances r_1 and r_2 from each slit to the screen. Thus we should consider the fresnel diffraction model for the fitting of the asymmetric double slit.

Similarly, we can consider the fresnel diffraction model for the single slit fitting. R^2 value for the second slit is 0.9890, which is less than the first slit. For a better fit, the Fresnel model approach was attempted. The results are shown in the figure below.

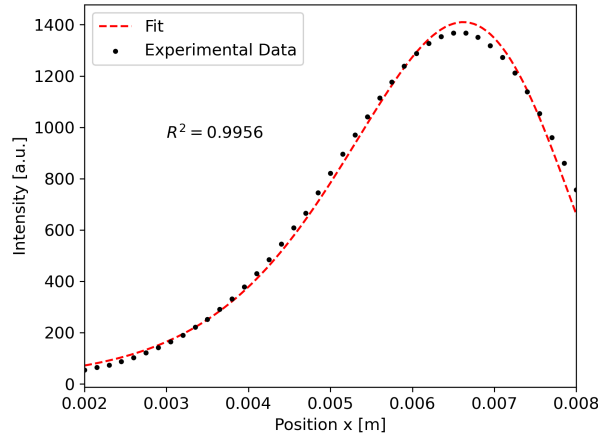


Figure 17. The diffraction pattern and the best fit of the single slit 2 for slit 14, with fresnel diffraction model.

The width for the slit 2 of double slit (that corresponds to Figure 17) was $d_2 = 103.9 \pm 17.2 \mu\text{m}$, and the width of the blocker slit was calculated as $w = 1.793 \pm 0.111 \text{ mm}$.

Using d_2 obtained from the Fresnel diffraction model, we can conduct a statistical test to determine if the two slits are of equal width. The Z-score for the difference between slit widths is calculated as follows:

$$\sigma = \sqrt{\frac{\sigma_1^2 + \sigma_2^2}{2}} = \sqrt{\frac{0.1^2 + 17.2^2}{2}} = \sqrt{\frac{295.85}{2}} \simeq 12.16 \text{ mm} \quad (13)$$

$$Z = \frac{|d_1 - d_2|}{\sigma} = \frac{|84.8 - 103.9|}{12.16} \simeq 1.57 \quad (14)$$

Therefore, the calculated Z-score is less than 1.96, so we cannot reject the null hypothesis that the two slits are of equal width. Therefore, we can conclude that the two slits are of equal width. Using this Fresnel model, we could get this result that is consistent with the result of bulb source experiment.

We did not consider the linewidth of the wavelength here, as it would require a time increase by the square of three halves of the current duration. While it is expected due to increased degrees of freedom, it is noteworthy that in laser double slit experiments where linewidth was considered, the R^2 value improved. Therefore, it can be anticipated that incorporating linewidth would result in a better fit than currently achieved.

C. Calculating the photon flux and single photon limit

Note that the process of determining the single photon limit was informed by referencing an exemplary report from the 2022 Intermediate Physics Experiment 1. [7]

1. Single photon limit

The both laser light source, and the bulb light source we used have a linewidth of wavelength. We can consider this as a uncertainty of momentum, as $\sigma_p = \frac{h\sigma_{\lambda_0}}{\lambda_0^2}$. According to the Heisenberg uncertainty principle, $\sigma_p\sigma_x \leq \frac{\hbar}{2}$. Hence we can write as:

$$\sigma_x \leq \frac{\hbar}{2\sigma_p} = \frac{\lambda_0^2}{4\pi\sigma_{\lambda_0}} \quad (15)$$

Using (15), we can calculate the uncertainty of the position x for each light source. For the laser light source, $\lambda_0 = 670$ nm, $\sigma_{\lambda_0} = 17.16$ nm, so $\sigma_x = 2081.72$ nm. For the bulb light source, $\lambda_0 = 567$ nm, $\sigma_{\lambda_0} = 23.1$ nm, so $\sigma_x = 1107.50$ nm.

2. In laser source: multiple photon regime

For the laser power 1mW that we used, about 10^{15} photons per second is produced. Considering the size ratio of source slit to the total area as $\sim 10^{-3}$, and assuming that the protons are uniformly distributed along the optical path line, their average distances are $c \times \frac{1s}{10^{15}} \sim 100$ nm. Since the uncertainty of the position for laser light source is $\lambda_0 = 670$ nm and it is greater than average distance, we can consider this experiment as a multiple photon regime.

3. In bulb source: single photon regime

The PMT's efficiency is approximately 4%, and the width of the channel is approximately 10 mm. [8] The width of the source slit is approximately 0.85 mm, so about 0.85% of the light passes through the source slit. About 600 signals are counted per second in PCIT for bulb power 5 (referred to Figure 9), so we can assume that about 10^6 photons pass through the source slit per second. Therefore, the average distance is $c \times \frac{1\text{sec}}{10^4} \sim 10^4$ m. This value is much greater than the uncertainty of the position, so we can consider this experiment as a single photon regime.

For the bulb power 5, about $\sim 10^4$ photons pass the first slit per second, as seen in Figure 9.

VI. CONCLUSION

In this lab, we aimed to investigate the wave-particle duality of light by conducting interference-diffraction experiment. In laser source with multi photon regime, we could find using the model with linewidth of wavelength shows the better fitting, comparing to the nonmonochromatic bulb source. In each experiment, we used the proper fitting model, especially using the fresnel model for the asymmetric double slit. In bulb source, we could find

that even in the single photon regime, it showed the interference–diffraction pattern, which concludes to the wave nature of light.

VII. BIBLIOGRAPHY

- [1] T. Young, “II. The Bakerian Lecture. On the Theory of Light and Colours,” *Philosophical Transactions of the Royal Society of London*, vol. 92, pp. 12–48, 1802, doi: 10.1098/rstl.1802.0004.
- [2] P. G. Merli, G. F. Missiroli, and G. Pozzi, “On the statistical aspect of electron interference phenomena,” *American Journal of Physics*, vol. 44, no. 3, pp. 306–307, 1976, doi: 10.1119/1.10184.
- [3] S. Eibenberger, S. Gerlich, M. Arndt, M. Mayor, and J. Tüxen, “Matter – wave interference of particles selected from a molecular library with masses exceeding 10000 amu,” *Physical Chemistry Chemical Physics*, vol. 15, no. 35, pp. 14696–14700, 2013, doi: 10.1039/c3cp51500a.
- [4] R. Rosa, “The Merli – Missiroli – Pozzi Two-Slit Electron-Interference Experiment,” *Physics in Perspective*, vol. 14, no. 2, pp. 178–195, 2012, doi: 10.1007/s00016-011-0079-0.
- [5] F. L. Pedrotti, L. S. Pedrotti, and L. M. Pedrotti, *Introduction to Optics*, 3rd ed. Upper Saddle River, NJ: Pearson, 2006.
- [6] “Two-Slit | TeachSpin — teachspin.com.” 2024.
- [7] D. of Physics and Astronomy, *Intermediate Physics Experiment: Report Writing Guide*. Seoul National University, 2024.
- [8] D. of Physics and Astronomy, *Intermediate Physics Experiment: Single Photon Interference Manual*. Seoul National University, 2024.